RoManSy 8, CISM-IFtoMM symposium
on Theory and Practice of Robots
and Manipulators, Poland
pp. 186-193

# PERFORMANCE EVALUATION OF FORCE/TORQUE FEEDBACK CONTROL METHODOLOGIES

Dieter Vischer and Oussama Khatib
Robotics Laboratory
Computer Science Department
Stanford University

## ABSTRACT

The paper focuses on the performance analysis of conceptually two different manipulator force/torque control methodologies: pure force/torque feedback control and position-based force/torque control methods. Force/torque control in the second scheme is achieved using a position or velocity inner loop, whose set point is specified by the force/torque outer loop. The basic argument for the use of position/velocity inner loops has been the collocation of (position) sensors and actuators. It has been argued that the achievable gains for the position/velocity inner loops will be higher than those that can be obtained with a direct force/torque feedback using the non collocated force/torque sensors. Assuming that higher gains can be obtained with a position/velocity loop, the crucial issue is to determine what effects the closure of the outer loop of force/torque feedback will have on the stability and performance of the overall system.

The primary concern is indeed the effective bandwidth of the system resulting from the closure of both loops of force/torque and position/velocity. The paper compares the two types of force/torque control methods on the basis of performance criteria involving stability, effective bandwidth, disturbance rejection, and backdriveability. The performance evaluation is conducted through both theoretical and experimental studies. The experimental support is a prototype link of ARTISAN instrumented with a new type of torque sensor.

## 1. INTRODUCTION

The work reported here is a part of a larger effort concerned with the development of a high-performance force controlled, ten degree-of-freedom manipulator and mini-manipulator system, ARTISAN, currently under development at Stanford University (Roth et al. 1988).

Force control has emerged as one of the basic means to extend robot capabilities in performing advanced tasks. A prerequisite to force control implementation is the manipulator ability to achieve precise control of joint torques. This ability, however, is considerably restricted by the nonlinearities and friction inherent in the actuator-transmission systems generally found in industrial robots. The wide use of position-based control is partly a natural result of the state-of-the-art in manipulator mechanical technology, which relies almost exclusively on the concept of joint position control.

The list of desirable properties of force controlled manipulator includes: high backdriveability, low friction, low effects of ripple torques and dynamic forces, low backlash, and small distributed elasticities (Colgate and Hogan 1989, and Eppinger 1987). While avoiding transmission nonlinearities, direct drive manipulators become increasingly massive and bulky with the increase in the number of degrees of freedom. The solution adopted for the actuation of ARTISAN has been to use brushless motors with a single stage low gear reduction system with torque sensing. Joint torque feedback is aimed at reducing

friction and transmission effects. The goal is to design for each joint, an independent, high bandwidth, robust torque servo controller.

Joint torque control is a simple (one-dimensional) case of the more general problem of end-effector force control. Force/torque control methodologies can be classified into the following two types:

- Pure force/torque feedback control methods;
- Position-based force/torque control methods (using inner loops of position or velocity feedback).

The performance of a force/torque control scheme is strongly dependent on the controller's achievable gains. The positive effect of sensor/actuator collocation on achievable gains has been the basic argument in favor of the use of inner loops of position/velocity feedback in force/torque control methods. However, even if higher gains can be achieved at the position/velocity loop, the crucial question to answer is: what effects the closure of the outer loop of force/torque feedback will have on the performance and stability of the overall system?

The paper presents a performance evaluation of the two above types of force/torque control methods. The performance criteria used in this evaluation involve stability, effective bandwidth, disturbance rejection, and backdriveability. The performance evaluation is conducted through both theoretical and experimental studies.

The experimental work was conducted on a prototype link of ARTISAN, which uses a newly designed torque sensor. With this sensor, torques are evaluated by distance measurements of the deflection in the sensor's structure using contact-less inductive transducers. This provides a substantial increase in accuracy over conventional strain gauge sensors, achieves higher mechanical robustness, and presents lower sensitivity to electrical noise. Although this study uses a one-link system as an experimental support, its conclusions have a clear impact on multi-link systems and end-effector force control.

## 2. PROTOTYPE LINK

The prototype link of ARTISAN, shown in Figure 1.a, uses a brushless dc motor, which is mounted at the base of the link in order to counterbalance the link's mass. The motor torque is transmitted in parallel through two single-stage low gear-reduction transmissions. A shaft encoder is located on the motor axis to measure the relative position between the link and the motor. The torque sensor is integrated in the gear, as shown in Figure 1.b Four inductive contact-free transducers, arranged in Wheatstone bridges, measure the deflection of the sensor structure. A detailed description of the dynamic modeling, the torque-control algorithms and the sensor used for the prototype link can be found in (Vischer and Khatib 1989).

The analysis of the transfer function from motor torque to measured torque at the sensor (which corresponds to the link torque) and the experimental frequency and step responses, as later presented in Figure 8, have shown the system to have a dominant second order behavior with weak damping.

The dominant dynamic behavior of the prototype link is illustrated in the simple mechanical model, shown in Figure 2. Static friction (Coulomb friction), dynamic friction, and motor ripple forces, which can be regarded as disturbance forces acting on the motor, are represented by the force $F_d$. $F_m$ is the motor force and $F_s$ the force measured at the sensor. The open-loop transfer function is

$$F_s = \frac{k_0\omega_0^2}{s^2+\omega_0^2}(F_m + F_d) \quad \begin{cases} k_0 = \frac{1}{1+\frac{m_m}{m_l}}; \\ \omega_0^2 = k_s(\frac{1}{m_l} + \frac{1}{m_m}); \end{cases} \tag{1}$$

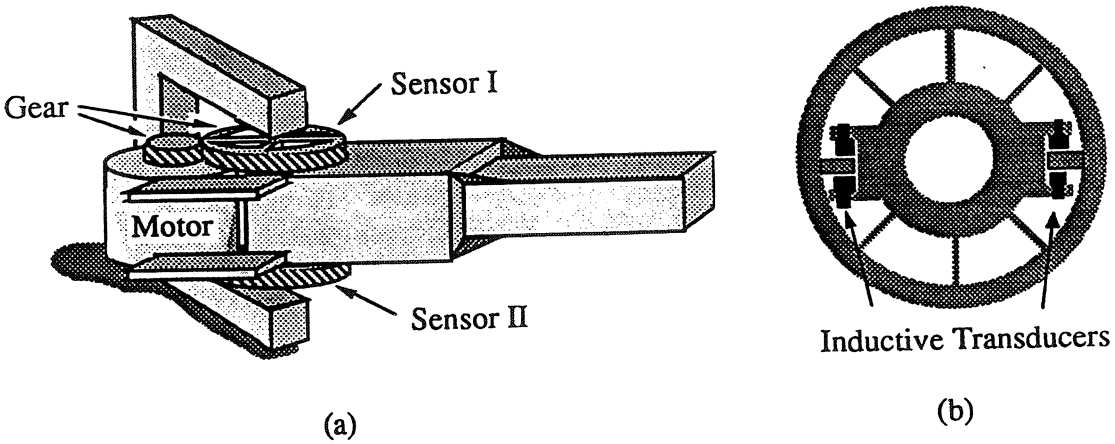


Figure 1: Prototype Link

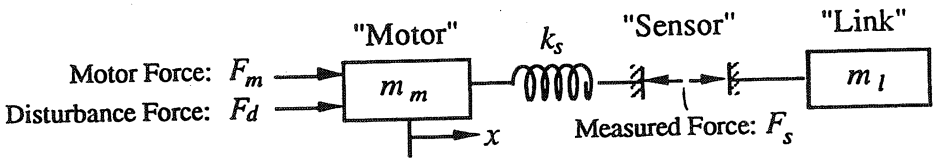


Figure 2: Mechanical Model

where $k_0$ is the open-loop gain and $\omega_0/2\pi$ the open-loop frequency, $f_0$. The transfer function for the constrained link, i.e., the link in contact with the environment, can be obtained from equation (1) by letting $m_l$ go to infinity. The open-loop gain and frequency of the link are given in Table 1.

## 3. PURE FORCE/TORQUE CONTROL

By "pure force control" we designate control methodes that use the error between the desired force $F_{des}$ and the measured force $F_s$ to control the motor torque $F_m$. Given the high open-loop frequency of the system under consideration, the most suitable type of controller is a lag controller. We simply select the integrator

$$F_m = F_{des} - K_I \int (F_s - F_{des}) dt; \tag{2}$$

where $K_I$ is the integral gain for a first evaluation.

## 4. POSITION-BASED FORCE/TORQUE CONTROL

The schematic of a position-based controller is shown in Figure 3. It consists of an inner position or velocity loop and an outer force servo control loop (Maples and Becker 1986).

Table 1: Link Parameters

| | | Free Link | Fixed Link |
|---|---|---|---|
| Open-Loop Gain | $k_0$ | 0.88 | 1 |
| Open-Loop Frequency | $f_0$ | 90 Hz | 85 Hz |

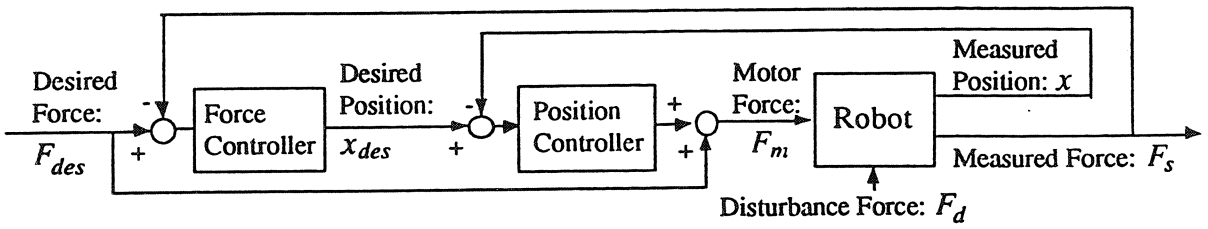


Figure 3: Position-Based Force/Torque Controller

Again, we select the simplest possible control algorithm. Here, the inner position servo loop controls the measured position $x$ to a desired value $x_{des}$:

$$F_m = F_{des} - K_P(x - x_{des}) - K_D\dot{x}. \tag{3}$$

The desired position is obtained from the outer force control loop as

$$x_{des} = -\tilde{K}_I \int (F_s - F_{des})dt. \tag{4}$$

Eliminating $x_{des}$ in equations (3) and (4), the control law for position-based force/torque control can be found as

$$F_m = F_{des} - K_I \int (F_s - F_{des})dt - K_P x - K_D\dot{x}; \tag{5}$$

with

$$K_I = \tilde{K}_I K_P. \tag{6}$$

The comparison of equation (2) and (5) shows that the difference between the two control schemes only lies on the addition of velocity and position feedback, $\dot{x}$ and $x$. The performance evaluation of the two schemes can thus be achieved by the evaluation of the impact of the addition of position and velocity feedback (or a spring and a damper) to a pure force control system.

In fact any position based force/torque controller (even in a multilink environment) can be interpreted as a superposition of a pure position controller and a pure force controller, since the (simple) transformation shown in equation (5) is allways possible for any combination of inner position loop and outer torque loop. In other words there allways exists a controller as presented in Figure 4 with exactly the same behavior as the controller of Figure 3. To understand position-based force or torque control, however, we believe that the interpretation shown in Figure 4 is much more clear (suitable).

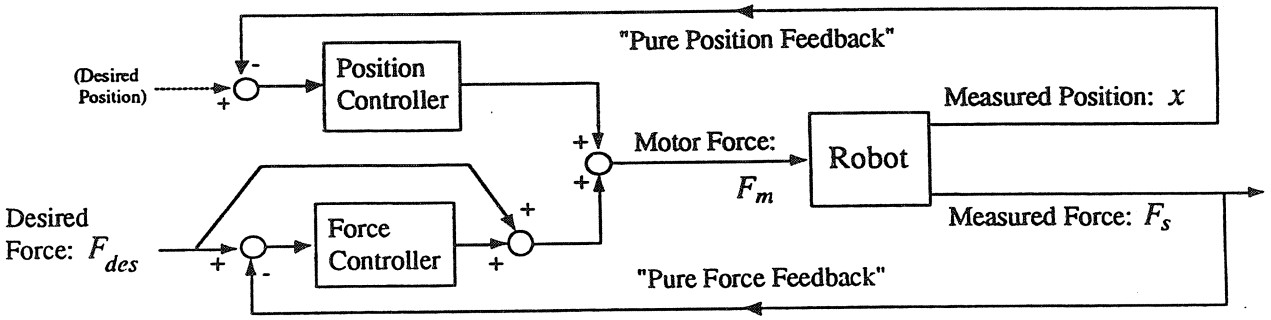


Figure 4: Superposition of Pure Position Control and Pure Force Control

The representation in Figure 4 allows for a better understandig of the "collocation argument" seemingly in favor of postion based force control. High gains on the position

controller are indeed possible but will result in a closed loop system which is dominated by the pure position feedback whereas the force feedback has little or no influance on the overall behavior. This clearly suggests that a low position gain (or no position feedback at all) is in fact desirable for good performance in force and torque control tasks.

## 5. OPEN LOOP CHARACTERISTICS

Force and torque control designs strongly depend on the stiffness of the considered robot arm. In theory, the collocation of sensors and actuators, i.e., encoders are directly mounted on motor shafts, predicts the position closed-loop bandwidth to be higher than the first resonance frequency of the system. In practice, however, the achievable bandwidth is dependent on a number of factors and can be much lower. For the prototype link of ARTISAN, for instance, the first resonance frequency has been found at about 90 Hz, while the achievable position bandwidth was limited to 12 Hz. The bandwidth limitation here is exasperated by the backlash and nonlinear stiffness of the transmission in the considered prototype.

With the assumption of a rigid structure, i.e., high open-loop frequency, we neglect the first resonance mode of the link and concentrate on the interactive effects between the position inner loop and the force/torque outer loop. The open-loop transfer function can be approximated by

$$(k_s \to \infty) \quad F_s \approx k_0(F_m + F_d). \tag{7}$$

## CLOSED LOOP CHARACTERISTICS

Using equations (5) and (7), the closed-loop transfer function for both, the position-based control and pure force control ($K_P = K_D = 0$) becomes

$$F_s = \frac{k_0(s^2 + K_I s)}{s^2 + k_0(K_I + \frac{K_D}{m_l})s + \frac{k_0 K_P}{m_l}} F_{des} + \frac{k_0 s^2}{s^2 + k_0(K_I + \frac{K_D}{m_l})s + \frac{k_0 K_P}{m_l}} F_d. \tag{8}$$

The closed-loop characteristic for the constrained link can be obtained by letting $m_l$ go to infinity:

$$(m_l \to \infty) \quad F_s = F_{des} + \frac{s}{s + K_I} F_d. \tag{9}$$

Equation (9) is independent of the position-feedback ($K_P$ and $K_D$). This shows that for a stiff sensor, manipulator, and environment, the contribution of any position feedback is negligible compared to the control action provided by the integration of the force error, when the link is constrained. For a free link, however, the difference of the two methodes becomes apparent.

Observing that the effective motor inertia $m_m$ is usually much smaller than the link inertia $m_l$ for low geared manipulators, such as the prototype, the closed loop transfer function for pure force control ($K_P = K_D = 0$) can be simplified to

$$(K_P = K_D = 0 \text{ and } m_m \ll m_l) \quad F_s \approx F_{des} + \frac{s}{s + K_I} F_d. \tag{10}$$

Equations (9) and (10) are identical and show that the pure force control method leads to almost identical closed-loop behavior for both cases of free and fixed link. In other words, the pure force servo has the desirable property of being insensitive to changes of the link inertia. This becomes particularly important for a multi-link system, where $m_l$ varies

with the manipulator configuration. In the case of position-based control the transfer characteristic, i.e., damping and bandwidth in equation(8) are strongly depending on $m_l$.

Figure 5 shows the frequency response of the open-loop system as described in equation (7) and compares it to the two force control schemes specified in equation (8). Figures 5.a, 5.c and 5.e display the transfer characteristic of each system, e.g., its capability of following a torque input, whereas Figures 5.b, 5.d and 5.f reflect their ability of reducing unknown disturbance forces originated at the transmission.

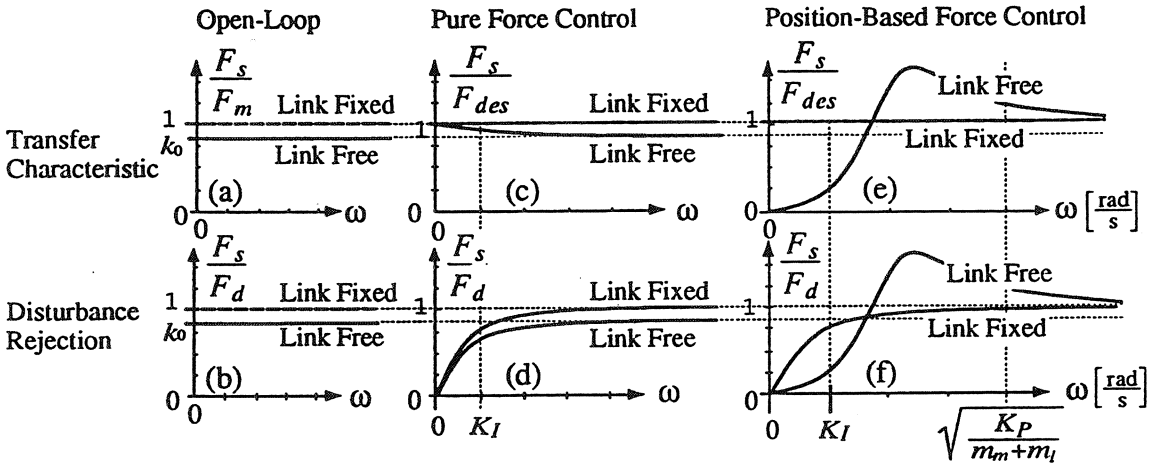


Figure 5: Closed-Loop Behavior

The pure force control (see Figure 5.d) provides an increased disturbance rejection below the frequency $K_I/2\pi$, with minor differences between free and fixed link (compare equations(9) and (10)). Both control methodes behave similarly for the fixed link, whereas for the free link the transfer characteristics associated with the position-based controller, shown in Figure 5.e, are very poor (worse than those of the open-loop, at high frequencies). Furthermore disturbances are amplified at high frequencies, as shown in Figure 5.f.

## 7. BACKDRIVEABILITY

A force/torque controlled robot should be able to move over an unknown and uneven surface, while maintaining a desired contact force. This situation can be analyzed by looking at the output impedance of the system, i.e., the transfer function from a disturbance $x_d$ to the measured force at the sensor $F_s$ as shown in Figure 6. A system's ability to reject such disturbances is described as its "backdriveability".

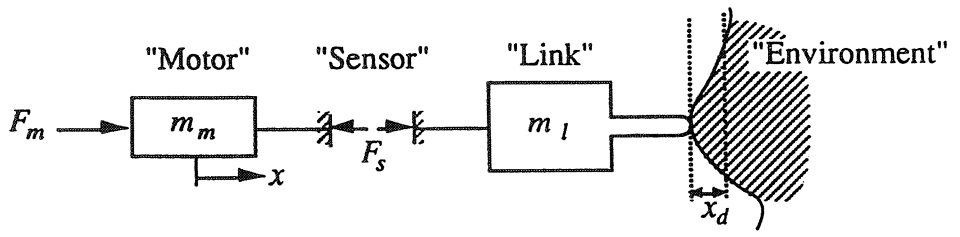


Figure 6: Sliding Over a Surface

Using the control law of equation(5), this transfer function is

$$F_s = \frac{s(m_m s^2 + K_D s + K_P)}{s + K_I} x_d. \qquad (11)$$

The Bode-diagrams of Figure 7 provide a comparison between the two control methods. It shows that both methods allow to improve the backdriveability for frequencies below $K_I/2\pi$. At higher frequencies, the position-based control performance are worse than the backdriveability of the open-loop system. The two control approaches provide roughly the same static friction reduction, and the link can be moved easily in closed-loop. However, the pure force control approach provides, in addition, a reduction of the effective inertia of the motor (more then twenty times for the prototype link). This makes the link feel very light. The position-based controller shows the same behavior when the link is moved slowly and carefully but for fast movements its weight seems to increase, since the controller fights any movement of the arm by applying high motor torques. We found this behavior to be a source of instability, since the link could easily go in limit cycles, as the motor torque is saturated.

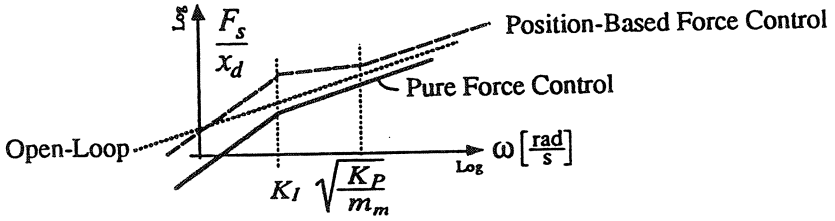


Figure 7: Backdriveability

## 8. EXPERIMENTS

Figure 8 shows some experimental results for the prototype link of ARTISAN. The motor inertia and link inertia are $0.027kg\ m^2$ and $0.23kg\ m^2$, respectively. A schematic of the controller we have used for our experiments is shown in Figure 9. A lookup table for the position-dependent torque-offset proved to be useful for our application. Furthermore two second order low-path filters with a cut off frequency of 70 Hz have been used for the desired torque, $T_{des}$, and the measured torque, $T_s$.

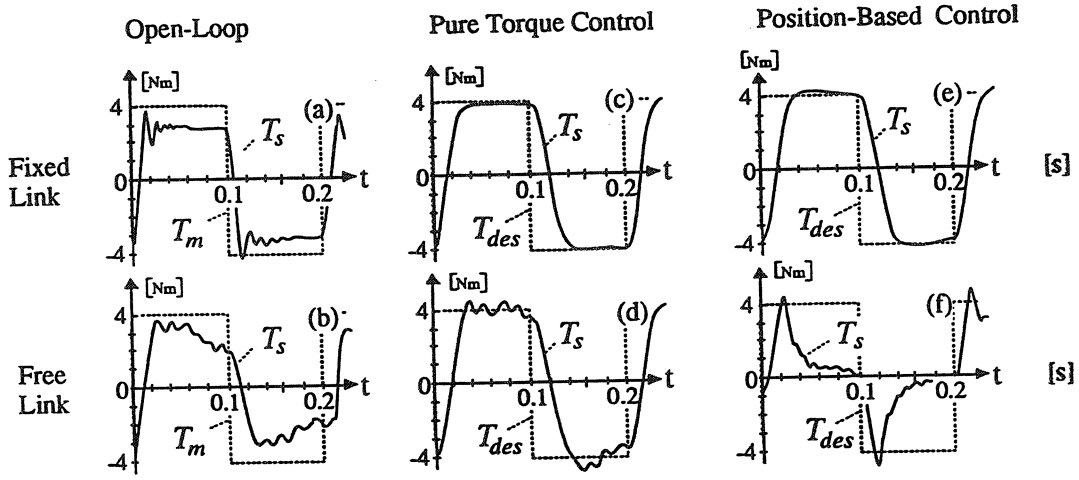


Figure 8: Experimental Results

The sampling frequency of the digital controller is 400 Hz. A simple lag controller is used for the pure torque servo with the control law

$$T_{out} = \frac{0.47z}{z - 0.997} T_{in}. \tag{12}$$

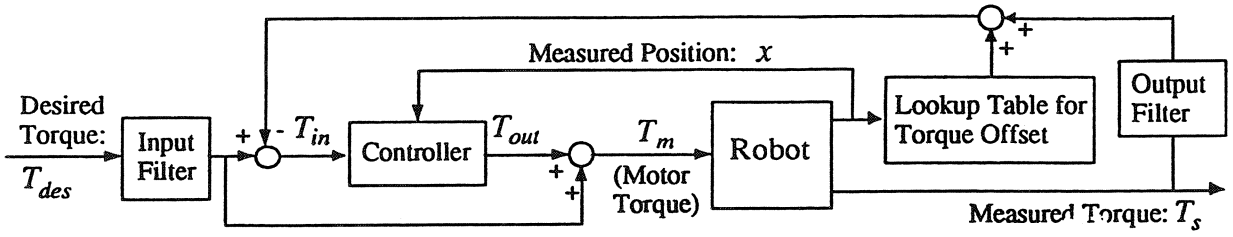


Figure 9: Controller Schematic

This resulted in a disturbance rejection bandwidth, $K_I/2\pi$, of 30 Hz. A comparison of the pure force controller (Figure 8.a,b) with the open-loop system (Figure 8.c,d) shows a significant reduction of the static error for the free and the fixed link (20 times improvement). The input filter prevents the command torque from exciting the first resonance mode (90 Hz) when the link is constrained. When the link is free, the resonance is excited by the cogging in the transmission system. The resulting ripples are reduced by the output filter before being fed back to the controller. The 10-90% rise time for the closed-loop system is less than 15 ms.

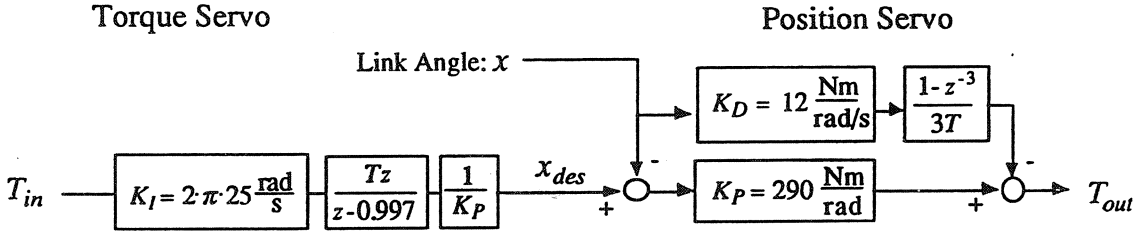


Figure 10: Position-Based Controller

The schematic for the position-based controller we have used are shown in Figure 10. The closed-loop frequency we were able to achieve for the position controller was 12 Hz. When we tried to close the outer torque loop, however, we found that even very small integral gains would lead to instability. Reducing the position bandwidth to 5 Hz allowed for an overall integral gain $K_I/2\pi$ of about 25 Hz. While the results for the fixed link (Figure 8.c,e,g) were satisfactory, the performance of the position-based controller has been very poor for the free link (Figure 8.f).

## 9. CONCLUSION

A position-based force/torque controller can be regarded as the result of the superposition of a pure force/torque controller and a pure position controller. Following the specified task, the control action is dominated by one of the two controllers. For tasks, where the link is in contact with the environment, the control action of the position feedback is negligible compared to the force feedback action. For free motion tasks or for compliant motion task where backdriveability is needed (or during transition to contact), the position feedback dominates the closed-loop behavior at high frequencies and results in poor performance (worse than the performance of the open-loop system).

The analysis and experimental results presented in this paper clearly show the inability of position-based controllers to provide force/torque control capabilities. On the other hand, these results demonstrate the effectiveness of the pure force/torque feedback approach for both cases of constrained and free links.

The performance limitations of the position-based approach can be expected to be yet more acute in the control of forces and moments at the manipulator end-effector. This is because of the method's sensitivity to variations of inertias and compliances, and to the additional dynamics associated with a multi-link system.

## ACKNOWLEDGMENTS

The financial support of SIMA, GM, and the Swiss NSF are acknowledged. We are thankful to Professors Bernard Roth and Kenneth Waldron and to Richard Voyles and David Williams, who have made valuable contributions to the development of this work.

## REFERENCES

Colgate, E., and Hogan, N., "An Analysis of Contact Instability in Terms of Passive Physical Environments," Proc. IEEE Int. Conf. on Robotics and Automation, Scottsdale, Arizona, 1989, pp. 404-409.

Eppinger, S.D., and Seering, W. P., "Understanding Bandwidth Limitations in Robot Force Control," Proc. IEEE Int. Conf. on Robotics and Automation, Raleigh, N.C., 1987.

Maples J.A., and Becker J.J., "Experiments in Force Control of Robotic Manipulators," Proc. Int. Conf. on Robotics and Automation, San Francisco, 1986.

Roth, B., Raghavan, M., Khatib, O., and Waldron, K., "Kinematic Structure for a Force Controlled Redundant Manipulator," Proc. Int. Meeting on Advances in Robot Kinematics, Ljubljana, Yugoslavia, 1988, pp. 62-66.

Vischer, D., and Khatib, O., "Design and Development of Torque-Controlled Joints," Experimental Robotics I, eds. Hayward, V. and Khatib, O., Springer-Verlag Berlin Heidelberg, 1990.

Vischer, D., and Khatib, O., "Performance Evaluation of Force/Torque Feedback Control Methodologies," 8th CISM-IFToMM Symp., Theory and Practice of Robots and Manipulators, Ro.Man.Sy '90, Cracow, Poland, July 1990.

Volpe, R., Khosla, P. "The Equivalence of Second Order Impedance Control and Proportional Gain Explicit Force Control: Theory and Experiments," Second Symposium on Experimental Robotics, Toulouse, 1991.